Computation Physics coursework 2

Raymund Francis Ibarrientos

October 2020

Introduction

The subject of this project is on star formation namely on the basic factors which decide its mass after formation. Stars are naturally created inside molecular clouds across the galaxy, especially in locations where the gas density is high. These high-density regions happen as a result of sudden changes in the density, such as from supernovae shock waves. Soon, these regions fragments into individual protostellar cores, which if enough mass is gained (at least $0.07M_{sun}$), then nuclear fusion occurs and a Zero-Age Main Sequence (ZAMS) star is born. Any less, then the protostellar core simply condenses into a brown dwarf. However, these molecular clouds experience several forces which constrains star formation, such as gas pressure, which can be overcome with sufficient density due to its own gravity.
This model of star formation uses the 1D Bondi mass form to test three basic variables - mass, gas density and sound speed. Though simplified to the point that accretion disks and planet formations are disregarded, the model still fulfils its point in examining the growth and mass distributions of the forming stars.

Bondi Mass derivations

Starting from this equation:

$$\frac{\partial}{\partial t}\rho + \frac{1}{r^2}\frac{\partial}{\partial r}(r^2\rho v) = 0 \tag{1}$$

By integrating this equation, it then forms into this equation:

$$r^2\rho v = const = \frac{\dot{M}}{4\pi} \tag{2}$$

Where $\dot{M}$ is the mass gained in a moment of time. After further derivations, one can finally reach this equation:

$$\frac{1}{2}(1 - \frac{1}{\mathcal{M}^2})\frac{\partial}{\partial r}(v^2) = -\frac{GM}{r^2}(1 - \frac{r}{r_s}) \tag{3}$$

Where $\mathcal{M}$ is the Mach number ($\mathcal{M} = \frac{v}{c_s}$). This equation shows
So when applying into a strongly supersonic region deep within the sonic radius, then the following conditions apply: $v >> c_s$ and $r << r_s$. Thus, when applying into the LHS and RHS of the equation respectively gives:

$$\lim_{v\to\text{inf}}\left(\frac{1}{\mathcal{M}^2}\right) = 0$$

$$\lim_{r\to 0}\left(\frac{r}{r_s}\right) = 0$$

Thus, by substituting them into equation 3, it results in:

$$\frac{1}{2}\frac{\partial}{\partial r}(v^2) = -\frac{GM}{r^2} \tag{4}$$

$$\implies \frac{1}{2}(v^2) = \int_0^r -\frac{GM}{r^2}\partial r \tag{5}$$

$$\implies \frac{1}{2}(v^2) = \frac{GM}{r} \tag{6}$$

$$\implies v^2 = \frac{2GM}{r} \tag{7}$$

$$\implies v = \left(\frac{2GM}{r}\right)^{1/2} \tag{8}$$

Note that with some rearranging of equation 7 as well as multiplying both sides by the mass of the particle itself, then the equation changes into $E_K E = E_G PE$, which indicates the transfer of gravitational energy to kinetic energy as it falls towards the core. Then, by applying it to equation 2:

$$r^2\rho\left(\frac{2GM}{r}\right)^{\frac{1}{2}} = \frac{\dot{M}}{4\pi} \tag{9}$$

$$\implies r^{2+-(1/2)}\rho = \frac{\dot{M}}{4\pi\sqrt{2GM}} \tag{10}$$

$$\implies r^{(3/2)}\rho = \frac{\dot{M}}{4\pi\sqrt{2GM}} \tag{11}$$

$$\implies \rho = \frac{\dot{M}}{4\pi\sqrt{2GM}}r^{-\frac{3}{2}} \tag{12}$$

$$\implies \rho = \frac{\dot{M}}{4\pi\sqrt{2GMr^3}} \tag{13}$$

From these equations and considering where the conditions necessary for them to apply, it can be interpreted that equation 8 is the speed of a particle moving towards the accreting core while equation 13 is the density of the gaseous core. A point of significance is that rearranging equation 13 to become $\dot{M} = 4\pi\rho\sqrt{2GMr^3}$ shows that the change of mass is strongly dependent on the mass of the core (assuming it to be treated as a point mass). This will ultimately lead to a cycle - the increase of mass will lead to it drawing yet more mass at an increasing rate up until there is no more material to draw or that process is somehow interrupted.
Another crucial equation is for the Bondi accretion rate, which calculates the mass change at a period of time as derived by Bondi 1952. The equation used is the following:

$$\begin{aligned} \dot{M}_{Bondi} &= f\frac{\pi G^2 M^2 \rho(r_s)}{c_s(r_s)^3} \\ where f(y) &= \left(\frac{2}{3-5\gamma}\right)^{\frac{5-3\gamma}{2(\gamma-1)}} \end{aligned} \tag{14}$$

Crucially, γ is the adiabatic factor, which is limited to $\gamma = 1$ at isothermal temperatures (developed by external factors such as radiation fields), and $gamma = \frac{5}{3}$ for fully adiabatic monatomic gas. At these conditions, then the limiting values are $f = e^{\frac{5}{3}}$ and $f = 1$ respectively, establishing that isothermic conditions allow for the strongest Bondi mass gain.
Finally, by letting $\gamma = 1.4$ (as in part-way close to the adiabatic monatomic gas conditons) and collecting the constants, then the final Bondi accretion rate equation used here becomes:

$$\dot{M} = C\left(\frac{M}{M_\odot}\right)^2\left(\frac{\rho(\infty)}{10^{-24}gcm^{-3}}\right)\left(\frac{c_s(\infty)}{10kms^{-1}}\right)^{-3} gs^{-1} \tag{15}$$

$$WhereC = f(1.4) \times \pi \times G^2 \times M_{sun}^2 \times 10^{-24} \times 10^3 = 1.4 \times 10^{11} \tag{16}$$

Cloud conditions and Bondi accretion rate

The key subject of this report is to examine how these conditions affect the masses of forming stars. To start however, one must assess what conditions the model simulation would be set.
Here, this subject is examined using a Monte-Carlo simulation of 1000 'protostars' with a uniform random mass between 0.001 and 0.01 $\dot{M}$. Each of them have a limited time of 3 Myrs to complete their accretion and formation through numerical integration with equation 14, upon which their masses were tallied and presented here through graphs. In addition, the gas density was set at $1.6\times10^{-20}g/cm^3$ and the sound speed to $10km/s$, both of which closely match the conditions of a typical molecular cloud. As an aside, table 1 and figure 1 shows an exponential growth to mass gain per 1Myrs as a protostar gradually increases in mass, with those located at the cloud core experiencing the highest mass gain and diffuse X-ray gas experiencing the lowest.

Location	Density M_p/cm^3	Sound Speed km/s
Diffuse X-ray gas	10^{-2}	10^2
Diffuse atomic gas	1	10
Molecular cloud	10^2	1
Cloud core	10^4	10^{-1}

Table 1: Gas phase

For additional convenience, rather than using linear scale graphs (see figure 2a), log-scale graphs with both population and mass log axes are used which display the distribution of masses at even binnings, allowing for ease of examination and crucially to. A line displaying the function $1/M_{sun}$ is also displayed at each logarithmic graph, which follows with the following derivation from Salpeter Law after a substantially long accretion time and so represents the Initial Mass Function.

$$\frac{dN}{dM} \propto M^{-2.35} \tag{17}$$

$$\implies \frac{dN}{dlog(M)} = M\frac{dN}{dM} \tag{18}$$

$$\left[\frac{dN}{dM} = M^{-2}\right] \tag{19}$$

$$\implies \frac{dN}{dlog(M)} = M(M^{-2}) \tag{20}$$

$$\implies \frac{dN}{dlog(M)} = M^{-1} \tag{21}$$

As a note, the upper limit for star mass is set at $150M_\odot$ as inferred from Weidner and Kroupa 2004 - though there may be no hard limit in reality, one could reliably set this as a soft limit at least for ZAMS stars. There are several other assumptions with this Monte-Carlo simulation, which heavily assumes that all the mass within the cloud is used to develop these stars and that they are allowed to form continuously through the given total timespan. In reality, a molecular cloud would quickly dissipate after the formation of a comparably few stars, as said stars would produce radiation which destroys the molecular compounds and so causing it to disintegrate and so deprive other stars from accreting additional material. Other factors which

may enhance or reduce the accretion effect, such as the protostar's magnetic field (Toropin et al. 1999) and rotation, are also not included into the model.
From the first effort, it seemed that these protostars had barely increased their mass into the minimum ignition mass (compare figures 2b and 3a). However, this is due to having considerably large time intervals of 0.1 Myrs - decreasing the time interval by a factor of 10 increases the accuracy of the results, resulting in a more substantial mass increase to the point that a substantial number of stars reached the upper mass limit. This is displayed at figures 3b, 3c and 3d, where the lattermost was considered to be the acceptable point of unity between the masses and the IMF function - decreasing the time interval sizes further would be too expensive in computing power for minimal gain. As for the content of that graph, it can then be seen that the masses begin to follow the IMF function by the 10^-2 mass mark, which is somewhat a deviation from the minimum accuracy of $10^{-0.4} M_{sun}$ (Salpeter 1955).
Next, while retaining the unity time interval, the next experiment is to affect the molecular gas density by tripling it and then reducing it to a third. The results for each is displayed as figures 4a and 4b respectively. As it can then be observed by the graphs, the effect of increasing the gas density has caused a significant quantity of extremely high-mass stars at the end of the total timespan. In contrast, reducing the gas density to 1/3 of its originally value resulted in it most, if not all, stars failing to exceed the minimum stellar fusion mass of $0.75 M_{sun}$ (or roughly 10^{-1}), meaning that a much longer timespan of accretion would be necessary for them to gather enough mass at all.

Conclusion

This project has shown the importance of at least a few major factors in star formation. From these results, it can then be seen that at a reasonable timespan, ZAMS stars over the mass 10^{-2} begin to match the IMF, thus making it an acceptable simulation of star formation. However, changing the gas density results in a substantial change in mass which either leads to a saturation of of high-mass stars or production of only brown dwarfs respectively. In addition, the model simulation has made several implied or direct assumptions which would have otherwise affected the final masses, from the availability of gas material, the effect of fully-ignited stars inside the cloud to the properties of these protostars themselves.

References

Bondi, H (1952). "On spherically symmetrical accretion". In: *Monthly Notices of the Royal Astronomical Society* 112, pp. 195–204. DOI: 10.1093/mnras/112.2.195.

Salpeter, E E (1955). "The Luminosity Function and Stellar Evolution." In: *Astrophysical Journal* 151, pp. 161–167. DOI: 10.1086/145971.

Toropin, Yu M et al. (1999). "Spherical Bondi Accretion onto a Magnetic Dipole". In: *The Astrophysical Journal* 517 (2), pp. 906–918. DOI: 10.1086/307229.

Weidner, C and P Kroupa (2004). "Evidence for a fundamental stellar upper mass limit from clustered star formation". In: *Monthly Notices of the Royal Astronomical Society* 348 (1), pp. 187–191. DOI: 10.1111/j.1365-2966.2004.07340.x.

Appendix

Figure 1: Relation of mass and mass-gain of star at particular conditions

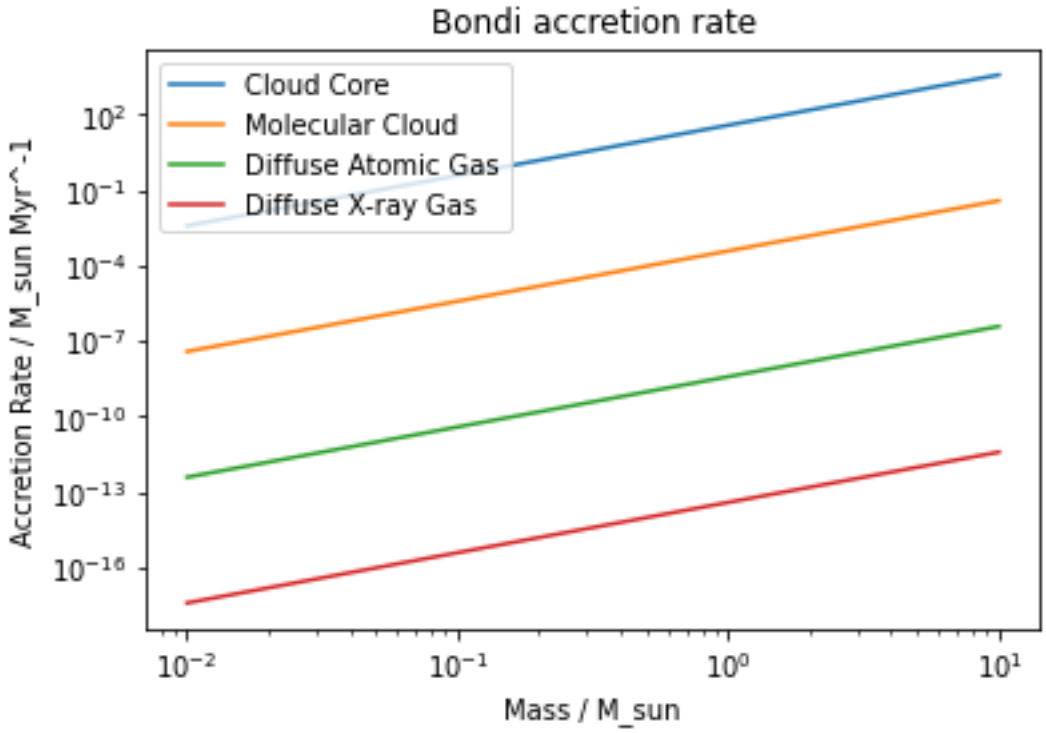

Figure 2: Initial mass of 'protostars'

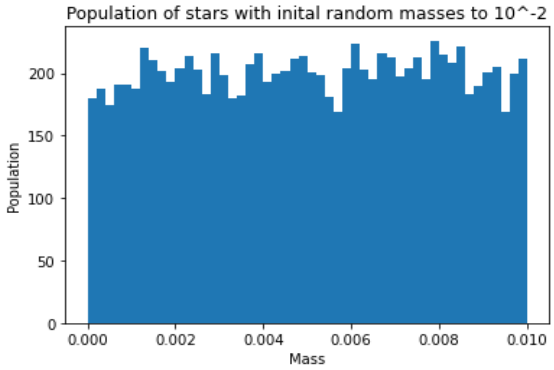

(a) Display of initial masses in linear scaling

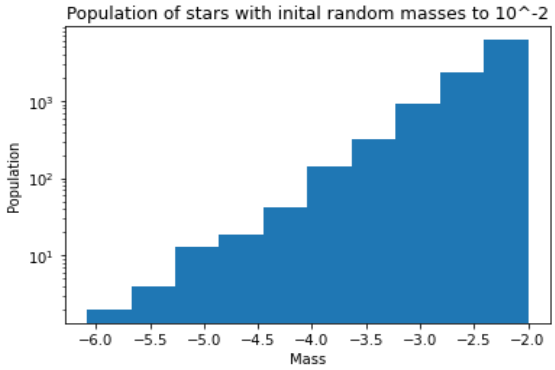

(b) Display of initial masses in log scaling with 1/M

Figure 3: Final masses with base parameters

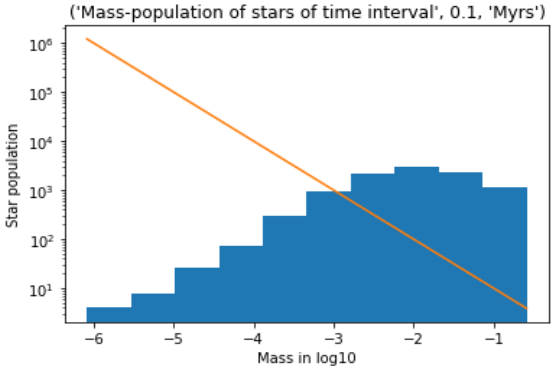

(a) Timestep = 100 kyrs

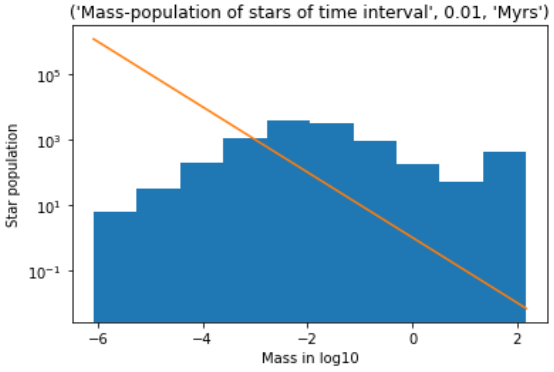

(b) Timestep = 10 kyrs

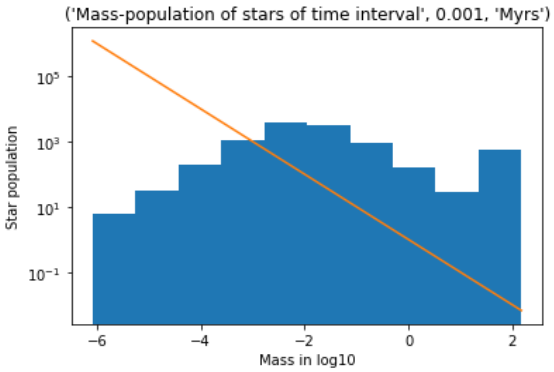

(c) Timestep = 1 kyrs

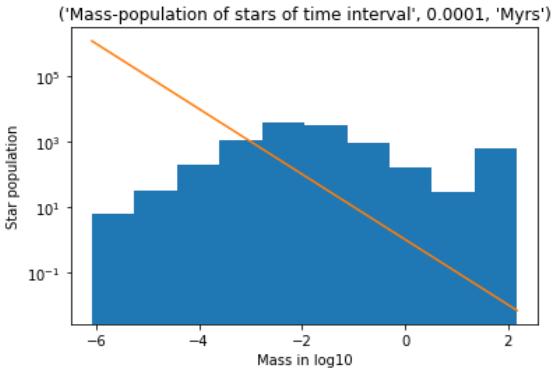

(d) Timestep = 0.1 kyrs

Figure 4: Final masses with altered gas density

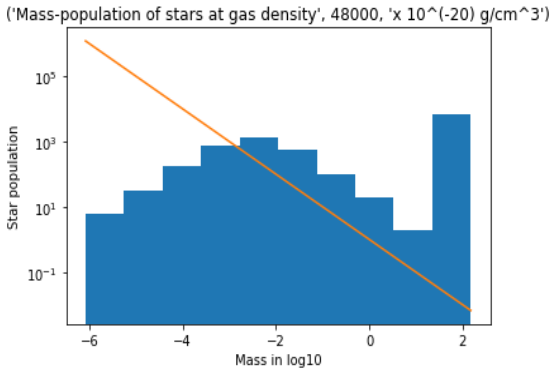

(a) Gas density = 3p

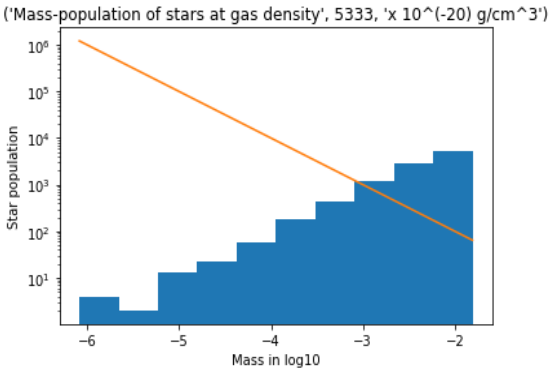

(b) Gas density = (1/3)p